Journal of Nuclear Medicine, published on June 24, 2021 as doi:10.2967/jnumed.120.259192

Title: **Feasibility, Biodistribution and Preliminary Dosimetry in Peptide-Targeted Radionuclide Therapy (PTRT) of Diverse Adenocarcinomas using ^{177}Lu-FAP-2286: First-in-Human Results**

Short running title: **^{177}Lu-FAP-2286 PTRT of Adenocarcinomas**

Authors: Richard P. Baum[1,2#], Christiane Schuchardt[1], Aviral Singh[1], Maythinee Chantadisai[1,3], Franz C. Robiller[1], Jingjing Zhang[1,4], Dirk Mueller[1], Alexander Eismant[1], Frankis Almaguel[1,5], Dirk Zboralski[6], Frank Osterkamp[6], Aileen Hoehne[6], Ulrich Reineke[6], Christiane Smerling[6], Harshad R. Kulkarni[1#]

#contributed equally

Affiliations: [1]Theranostics Center for Molecular Radiotherapy and Molecular Imaging, Zentralklinik Bad Berka, Bad Berka, Germany; [2]CURANOSTICUM Wiesbaden-Frankfurt, Center for Advanced Radiomolecular Precision Oncology, Wiesbaden, Germany; [3]Faculty of Medicine, Chulalongkorn University, King Chulalongkorn Memorial Hospital, Bangkok, Thailand; [4]Yong Loo Lin School of Medicine, National University of Singapore, Singapore, 117597, Singapore; [5]Loma Linda University, Loma Linda, USA; [6]3B Pharmaceuticals GmbH, Berlin, Germany

First author: Prof. Dr. med. Richard P. Baum, CURANOSTICUM Wiesbaden-Frankfurt, Aukammallee 33, 65191 Wiesbaden, Germany; Telephone number +4961195006815; Fax number +49611577587; Email – baumrp@gmail.com

Corresponding author: Harshad R. Kulkarni, Zentralklinik Bad Berka, Robert-Koch-Allee 9, 99437 Bad Berka, Germany; Telephone number +493645852101; Fax number +493645853547; Email – harshad.kulkarni@zentralklinik.de

Word Count: 5993

ABSTRACT

Fibroblast activation protein (FAP) is a promising target for diagnosis and therapy of numerous malignant tumors. FAP-2286 is the conjugate of a FAP-binding peptide, which can be labeled with radionuclides for theranostic applications. We present the first-in-human results using ^{177}Lu-FAP-2286 for peptide-targeted radionuclide therapy (PTRT). **Methods:** PTRT using ^{177}Lu-FAP-2286 was performed in 11 patients with advanced adenocarcinomas of pancreas, breast, rectum and ovary after prior confirmation of uptake on ^{68}Ga-FAP-2286/-FAPI-04- PET/CT. **Results:** Administration of ^{177}Lu-FAP-2286 (5.8 ± 2.0 GBq; range, 2.4–9.9 GBq) was well tolerated, with no adverse symptoms or clinically detectable pharmacologic effects being noticed or reported in any of the patients. The whole-body effective doses were 0.07 ± 0.02 Gy/GBq (range 0.04 – 0.1). The mean absorbed doses for kidneys and red marrow were 1.0 ± 0.6 Gy/GBq (range 0.4 – 2.0) and 0.05 ± 0.02 Gy/GBq (range 0.03 – 0.09), respectively. Significant uptake and long tumor retention of ^{177}Lu-FAP-2286 resulted in high absorbed tumor doses, e.g., 3.0 ± 2.7 Gy/GBq (range 0.5 – 10.6) in bone metastases. No grade (G) 4 adverse events were observed. G3 events occurred in 3 patients – 1 pancytopenia, 1 leukocytopenia and 1 pain flare-up; 3 patients reported pain-response. **Conclusions:** ^{177}Lu-FAP-2286 PTRT, applied in a broad spectrum of cancers, was relatively well-tolerated with acceptable side effects and demonstrated long retention of the radiopeptide. Prospective clinical studies are warranted.

***Keywords*:** Fibroblast activation protein, ^{177}Lu-FAP-2286, peptide-targeted radionuclide therapy (PTRT), first-in-human, adenocarcinoma

INTRODUCTION

In recent years, the tumor microenvironment (TME) has gained interest as a therapeutic target in the treatment of cancer. A substantial part of the tumor can be made up by TME: in pancreatic ductal carcinoma, for example, it has been reported to form up to 80% of the tumor mass (*1*). Cancer-associated fibroblasts (CAFs) are an integral part of the TME and present abundantly in the tumor stroma of tumor entities such as breast and colon cancer (*2*). A marker protein of CAFs is fibroblast activation protein (FAP), a type II transmembrane cell surface serine proteinase belonging to the dipeptidyl peptidase (DPP) family (*3*). FAP, which was discovered more than 30 years ago, is overexpressed on CAFs of over 90% of epithelial tumors such as breast, colorectal, lung, ovarian, and pancreatic adenocarcinomas. Since FAP expression in normal tissue is limited, it has been identified as a pan-tumor target for the potential treatment of cancer (*4*). In cancer indications of mesenchymal origin, notably sarcoma and mesothelioma, FAP is expressed on the tumor cells in addition to CAFs (*5,6*). FAP expression is also present in chronic inflammatory diseases like rheumatoid arthritis and osteoarthritis as well as during cardiac remodeling after myocardial infarction (*7,8*).

The first approach of using FAP as a target in cancer treatment applied the monoclonal antibody sibrotuzumab was tested in both an unconjugated and ^{131}I- conjugated format for the treatment of colorectal cancer (*9,10*). Other approaches targeting FAP including bispecific antibodies or antibody fragment constructs, chimeric antigen receptor (CAR) T cells, and antibody drug conjugates are currently being pursued, most of which are in preclinical development or phase 1 clinical trials (*6,11*). Small molecule FAP inhibitors (FAPI) have also been discovered (*12*) and conjugated with radioactivity to yield excellent imaging agents suitable for a variety of cancer indications (*13,14*).

FAP-2286 is comprised of a peptide that potently and selectively binds to FAP and 1,4,7,10-Tetraazacyclododecane-1,4,7,10-tetraacetic acid (DOTA) attached via a linker (*15*). FAP-2286 and its metal complexes had potent affinity to human FAP protein (K_D, 0.4-1.4 nM), whereas limited off target activity was seen against closely related family members. Labeled with the therapeutic β-particle emitting radionuclide ^{177}Lu, FAP-2286 had potent anti-tumor activity in FAP expressing HEK-293 xenografts after a single intravenous dose (*16*).

Here we report our initial experience with FAP-2286 radiolabeled with the beta-particle emitter 177-lutetium (^{177}Lu) for the treatment of patients with advanced metastatic cancers after exhaustion of all other treatment options.

MATERIALS AND METHODS

Patients and Regulatory Issues

PTRT with ^{177}Lu-FAP-2286 was administered as a therapy with palliative intent, after pre-therapeutic confirmation of FAP expression of the metastases using ^{68}Ga-FAP-2286 PET/CT (n = 9)/-FAPI-04 (n = 2) PET/CT (tumor-to-background (liver) ratio of standardized uptake values >3, Supplemental Table 1), to 11 patients (Pts) with progressive and metastatic adenocarcinoma of the pancreas (n=5, Pts 1-5), breast (n=4, Pts 6-9), ovary (n=1, Pt 10) and rectum (n=1, Pt 11), in accordance with paragraph 37 of the updated Declaration of Helsinki, ‘‘Unproven Interventions in Clinical Practice,’’ and in accordance with the German Medical Products Act (AMG §13 2b). Pts 5 and 9 were screened using ^{68}Ga-FAPI-04 PET/CT for screening before therapy, whereas all the other patients had been screened by ^{68}Ga-FAP-2286 PET/CT. The cut-off of tumor-liver ratio of >3 on screening ^{68}Ga- FAP-2286 PET/CT was to ensure a significant FAP expression of metastases as an essential criterion for patient selection, also considering the low physiological liver uptake. PTRT was performed at Zentralklinik Bad Berka (Bad Berka, Germany). The study was performed in accordance with German regulations (Federal Agency for Radiation Protection) concerning radiation safety and was approved by the institutional review board. All patients signed a detailed informed consent form before undergoing the treatment, as well as consented to the use of their anonymized clinical data for scientific purposes.

The patients were followed up until death or up to progression following initiation of PTRT. Metastases were present in the following localizations: lymph node (n=6), lung (n=3), pleura (n=1), peritoneum (n=3), liver (n=7), bone (n=5) and diffusely in bone-marrow (n=2). 6 patients had been operated for their primary tumor, 8 had been treated with chemotherapy, 3 with other

radionuclide therapies, 2 with check-point inhibitors and 1 with a poly(ADP-ribose)polymerase (PARP)-inhibitor. Pt 9 had concluded chemotherapy 4 weeks prior to start of PTRT, and Pts 2 and 7, two weeks before PTRT. Pt 10 received the last nivolumab administration 4 weeks prior. Two patients (Pts 1 and 3) categorically refused any other treatment like surgery or chemotherapy, and Pt 5 was deemed unfit for chemotherapy. Patients' characteristics are listed in Table 1.

Radiolabeling of 3BP-2286 with ^{68}Ga

The peptide FAP-2286 was labeled with ^{68}Ga using the NaCl based labeling procedure as previously described (*17*). For the automated radiopharmaceutical production, a Modular-Lab PharmTracer Modul (Eckert&Ziegler) was used (*18*). In detail, up to four ^{68}Ge/^{68}Ga generators were eluted and the eluate (1.2 – 2.6 GBq) was passed through a preconditioned SCX-cartridge. The ^{68}Ga collected was subsequently eluted using 0.5 mL of 5M NaCl, spiked with 12.5 µL 5.5 M of HCl. The ^{68}Ga-eluate of the SCX-cartridge was then added to a solution of 150 µg FAP-2286, 5 mg L- ascorbic acid and 1.2 mg of L-methionine dissolved in 350 µl 1M sodium acetate buffer (adjusted with HCl and acetic acid to pH=4.5) and 2.3 mL of water for injection. The reaction mixture was heated to 95°C for 8 minutes. After labeling the mixture was diluted with 2 mL of water for injection, neutralized using 2 mL of sterile sodium phosphate buffer (BRAUN-Melsungen) and sterile filtered. Samples were obtained for quality control, endotoxin test and test for sterility. The radiolabeling yield and the radiochemical purity were determined by iTLC and HPLC, respectively.

Radiolabeling of FAP-2286 with ^{177}Lu

Automated labeling was carried out using a PiRoSyn-synthesis module (Sykam, Fürstenfeldbruck, Germany) (*19*). To a solution of ^{177}Lu in 300 µl 0.05M HCl, a solution of 10 mg L-ascorbic acid, 5 mg L-methionine and FAP-2286 (20 MBq ^{177}Lu per µg of FAP-2286) in 1 ml of 1 M sodium acetate buffer (adjusted with HCl to pH=5.5) was added. The mixture was heated to 95°C for 35 minutes. The mixture was diluted with 0.9 % saline solution and sterile filtered. Samples were tested for quality, endotoxins, and sterility. Radiochemical purity, as determined by thin-layer and high-performance liquid chromatography, was consistently higher than 98%.

Treatment protocol

^{177}Lu-FAP-2286 was administered intravenously over 5-10 minutes. All patients presented with aggressive disease and high tumor load, primarily necessitating high dosages (radioactivities to be administered) for tumor control. The injected activity was adapted, if necessary, based not only on the patient's clinical condition, hematologic and renal function, but also the tumor distribution, i.e., in case of red marrow involvement. For e.g., a pre-existing grade (G) 2 anemia necessitated reduction of the radioactivity to be administered. When the patient consented and their condition allowed for further treatment, additional cycles were administered 8 weeks later. 1 patient received a single cycle, 9 patients received 2 cycles, 1 patient received 3 cycles (Supplemental Table 2).

For prevention of nausea, 3 mg granisetron injected intravenously prior to ^{177}Lu-FAP-2286 administration was employed. For adequate hydration, 1L of a balanced electrolyte solution was administered for 2h after radiopharmaceutical application, with addition of 20 mg furosemide.

Symptoms and vital parameters were monitored before, during, and after treatment. Patient characteristics, tumor features, and all previous treatments were documented. Complete blood count (CBC), liver and kidney function tests, creatine kinase, uric acid, electrolytes as well as tumor-associated markers including carcinoembryonic antigen (CEA), carcinoma antigen 15-3 (CA 15-3), carbohydrate antigen 19-9 (CA 19-9), and carbohydrate antigen 125 (CA-125) were determined before and in follow-up after each PTRT. Hematologic toxicity was graded according to Common Terminology Criteria for Adverse Events (CTCAE) version 5.0 (*20*).

Scintigraphy and SPECT/CT Imaging

The kinetics of ^{177}Lu-FAP-2286 were determined based on planar whole-body scintigraphy studies (anterior/posterior) and SPECT/CT 18 – 46 hours after administration of the radiopharmaceutical. Planar scintigraphy was acquired using a Spirit DH-V dual-head g-camera (Mediso, Germany), medium-energy general-purpose collimator, 15% energy window, 208-keV peak, and 15 cm/min speed. SPECT/CT was performed using a Siemens Symbia T camera system (Siemens Healthcare GmbH, Erlangen, Germany) with the following settings: MELP collimator, peak at 113 keV and 208 keV (15% energy windows and 20% upper and lower scatter window), 128x128 matrix, 32 projections with 30s per step, body contour.

Dosimetry protocol

At least five serial planar whole-body scintigraphies and one regional SPECT/CT were acquired per patient starting from 0.5h (immediately after therapeutic administration and before bladder voiding) post injection (p.i.). Since the patients were not allowed to empty the bladder

before the first scan, the total body counts acquired immediately after the injected activity were defined to be 100% of the administered activity. Total body counts on the subsequent scans were expressed as fractions of injected activity (%IA). Regions of interest (ROI) were drawn manually over the source regions over the acquired scintigraphy images, which were then analysed using the software of the HERMES system (Hybrid Viewer, Hermes Medical Solutions, Stockholm, Sweden). Source regions were defined as organs and metastases showing significant specific uptake, which could be clearly delineated on each post therapy scan. ROIs were selected by the same physicist, in collaboration with a nuclear medicine physician, who selected the suitable lesions for dosimetry (i.e., lesions with the highest uptake in the respective organ). As representative tumor lesions for dosimetry, bone and liver metastases were chosen due to their accurate localization and measurability on whole-body and SPECT/CT scans as well as high frequency of bone metastases. Lymph node and peritoneal lesions are limited by overlap on whole-body scans. The kinetics of whole body and source organs were determined based on this ROI analysis. The SPECT/CT scans were reconstructed and quantified using the HERMES SUV SPECT software (HERMES Medical Solutions, Stockholm, Sweden). After segmentation, the SPECT activity of source regions was used to scale the time-activity curves obtained from planar imaging. In the next step, these time-activity curves were fitted to mono- or bi-exponential functions to calculate effective half-lives and the time-integrated activity coefficient (ORIGIN PRO 8.1G, OriginLab Corporation, Northampton, USA). Mean absorbed organ and tumor doses

were finally estimated using OLINDA 2.0. The ICRP 89 adult model and the spheres model were used for normal organs and tumor lesions, respectively (both included in OLINDA 2.0). Volumes of normal organs and tumor lesions were obtained by the latest CT of the patient to adapt the model to individual organ and tumor volumes.

Dosimetry estimations were performed in 10 treatment cycles - in 4 patients (Pts 1, 4, 5 and 10) for a single cycle, and in 3 patients (Pts 6, 7 and 8) each for 2 cycles. Post-therapy scans were acquired at defined mandatory time points – immediately, 2-3 hours, and 1, 2 and 3 days – as well as, when the patient's condition allowed doing so, a further delayed scan up to 10 days post injection. Analysis was performed in accordance with our previously described protocol (*21*). Time-dependent activity in kidneys and metastases (n=14, 13 osseous and 1 hepatic) was determined by drawing regions of interest on serial ^{177}Lu-FAP-2286 whole-body scans after therapy. Mean absorbed dose to the red marrow was estimated from activity in the blood in 4/10 estimations, when the general condition and vein characteristics of the patient allowed doing so, as this requires multiple blood samples. In the other 6/10 estimations, it was determined based on whole-body activity distribution.

Clinical, Radiologic, and Laboratory Follow-up

Patient records were reviewed for any incidence of hematologic, gastrointestinal, renal, hepatic, or other adverse events, grade (G) was assigned according to CTCAE v5.0. Circumstances that resulted in cessation or delay in treatment were documented. Changes in circulating tumor markers were also recorded. All patients were systematically followed up after therapy by determining relevant laboratory parameters every 2 weeks. Baseline ^{68}Ga-FAP-2286-

PET/CT and contrast-enhanced CT or MRI were performed at a mean of 2 days (range 1-7 days) before the first PTRT cycle. To determine treatment efficacy, CT/MRI was performed in all patients, and ^{68}Ga-FAP-2286-PET/CT (except in Pt 5) in 10 patients, at 6-8 weeks after 1st therapy cycle. Pt 8 underwent restaging at 8 weeks after the 3rd therapy cycle using ^{68}Ga-FAP-2286-PET/CT.

RESULTS

Tolerability

The mean ± standard deviation of the administered amount of FAP-2286 was 290 ± 100 μg (range, 120–495 μg). The mean administered activity was 5.8 ± 2.0 GBq (range, 2.4–9.9 GBq). There were no adverse or clinically detectable pharmacologic effects in any of the 11 patients. No significant changes in vital signs or the results of laboratory studies, concerning immediate adverse events, were observed. Pts 4 and 6 reported a significant improvement in pain after treatment, requiring less morphine; Pt 5 had an improvement of his physical capacity and self-reported quality of life after treatment, in addition to pain relief.

Post-therapeutic ^{177}Lu-FAP-2286 whole-body scans and SPECT/CT

Visual analysis of post-therapy whole-body scans and SPECT/CT demonstrated significant uptake and retention of the ^{177}Lu-FAP-2286 in tumor lesions on delayed imaging (performed 72 h to 10 days post-injection) in all patients (SUV of ^{177}Lu-FAP-2286 in tumor lesions are displayed in Supplemental Table 3, and those of kidneys in Supplemental Table 4; representative examples are shown in Figs. 1 and 2; and the whole-body scans of patients 1-3, 5 and 7-11 in the supplemental figure 1). The initial biodistribution of the radiopharmaceutical was identical to the pre-therapeutic ^{68}Ga-FAP-2286 PET/CT.

Dosimetry

Dosimetric parameters, specifically effective half-life and mean absorbed dose to whole-body, kidneys and red marrow (Supplemental Table 5), as well as metastases (Supplemental Table 6), expressed as mean ± SD, were determined following ^{177}Lu-FAP-2286 administration

(Supplemental Table 7 enlists the dose estimations in all organs). The effective half-lives (in hours) were as follows: whole-body 35 ± 9 (range 25 – 48), kidneys 81 ± 51 (range 30 – 161), and bone metastases (n=13) 44 ± 25 (range 21 – 120) with mean absorbed doses for whole-body: 0.07 ± 0.02 Gy/GBq (range 0.04 – 0.1), for kidneys: 1.0 ± 0.6 (range 0.4 – 2.0), for red marrow: 0.05 ± 0.02 (range 0.03 – 0.09), and for bone metastases: 3.0 ± 2.7 (range 0.5 – 10.6). The effective half-life and mean absorbed dose in 1 liver metastasis (in Pt 4) were estimated to be 32 hours and 0.4 Gy/GBq, respectively.

Adverse events

Clinical adverse events included G1 short-term and self-limiting headache in 4 patients (Pts 3, 7, 9, 10) within 12 hours after treatment, which was moderate (G2) in 1 patient (Pt 9). There was severe flare-up of abdominal pain (G3) with nausea and vomiting after the second cycle in Pt 2. Incidentally, this patient had reported significant reduction in breathing-related pain in the left side of the back after the 1st cycle.

New anemia occurred after PTRT in 3 patients (G1 in Pts 1 and 4, G2 in Pt 11). Worsening of a pre-existing G1 anemia to G2 was noted in 2 patients (Pts 5 and 7) after the 2nd cycle. After the 3rd cycle, Pt 8 experienced G3 pancytopenia (from pre-existing G1-2), requiring packed red cell transfusions and granulocyte colony stimulation factor. Pre-existing leukocytopenia worsened from G1 to G2 in Pt 5 and from G2 to G3 in Pt 6. After PTRT, there was leukocytosis (non-G3) in 4 patients (Pts 3, 4, 7 and 11), which was noted after the 1st cycle in Pts 3, 7 and 11, and was reversible. In Pt 4, however, it occurred after the 2nd cycle and persisted until death 8 weeks later. Interestingly, in Pt 9, the leukocyte counts normalized (from pre-existing G1

leukocytopenia) and the absolute thrombocyte count improved (G1 unchanged) at 6 weeks after the 1st PTRT cycle (Table 2 and Supplemental Table 8).

Suffering from pre-existing chronic renal insufficiency G2, Pt 6 had episodes of acute deterioration of renal function after the first and second PTRT cycle, which were determined to be pre-renal. In both instances, renal function returned to normal within 4 weeks and the glomerular filtration rate remained consistently above 30 ml/minute. There was no significant change in renal parameters in the rest of the patients. The hepatic function parameters, uric acid, electrolytes, and creatinine kinase levels were unaffected by PTRT.

Outcome after PTRT

Evaluation according to Response Evaluation Criteria in Solid Tumors (RECIST) 1.1 in all patients at 6-8 weeks after 1st PTRT cycle revealed stable disease in 2 patients (Pts 8 and 9) and progression in the other 9 patients (Table 3). The findings also correlated with circulating tumor markers (Supplemental Table 9) and with ^{68}Ga-FAP-2286 PET/CT (performed in 10 patients). Due to marked disease progression, no further PTRT was administered to Pt 11. In Pt 6, ^{68}Ga-FAP-2286 PET/CT revealed a mixed response, i.e., remission of the diffuse bone metastases, but overall disease was progressive with evidence of new hepatic lesions (Fig. 2). Pt 8 demonstrated progression at 8 weeks after the 3rd PTRT cycle. 6 patients died due to disease progression 2 to 8 months after their initial PTRT (Table 3). 1 patient died due to suicide and 1 due to pneumonia.

DISCUSSION

This retrospective report provides the first evidence for feasibility of theranostics of diverse advanced adenocarcinomas using the novel radiolabeled peptide ^{177}Lu-FAP-2286. PTRT was

performed on a compassionate use basis in end-stage pancreatic, breast, ovarian and colorectal cancer patients after exhaustion of the treatment options, whereby 2 patients had strictly refused any other treatment, and 1 was deemed unfit for chemotherapy. The first-in-human use demonstrated a favorable safety profile with few manageable serious adverse events.

Pancreatic, breast, ovarian and colorectal adenocarcinomas and their metastases have been demonstrated to be FAP-positive on PET/CT (*22*). In our patient cohort, FAP expression was confirmed in these malignancies on PET/CT using ^{68}Ga-FAP-2286/-FAPI-04. Biodistribution images post-therapy revealed not only significant tumor uptake of ^{177}Lu-FAP-2286, but also long retention of the radiopharmaceutical in all patients. In contrast, biodistribution studies with small molecule based FAPI-based tracers, notably FAPI-02 and 04, revealed an earlier tumor washout and a correspondingly short tumor retention time (*14*), thereby limiting their therapeutic potential when conjugated to longer lived therapeutic radionuclides such as ^{177}Lu. Thus, the use of shorter-lived radionuclides for therapy using FAPI-based tracers was suggested (*19*). The longer tumor retention of FAP-2286, on the other hand, allows the use of therapeutically effective longer-lived radionuclides for therapy (including ^{177}Lu and ^{225}Ac).

This was further corroborated by dosimetric studies. Comparison of ^{177}Lu-FAP-2286 to other radiopharmaceuticals previously reported to be effective (i.e. ^{177}Lu-DOTATATE for neuroendocrine tumors (*23*) and ^{177}Lu-PSMA-617 for prostate cancer (*24*) shows comparable absorbed doses for whole body, bone marrow, and kidneys (*21,25,26*). Notably, the kidney absorbed dose delivered by ^{177}Lu-FAP-2286 when used without renal protection was comparable to that of ^{177}Lu-PSMA-617 and to that delivered by ^{177}Lu-DOTATATE when co-administered

with Lys/Arg for renal protection (1.0 (range 0.4 – 2.0) Gy/GBq vs 0.99 (range 0.45 – 1.6) Gy/GBq vs 0.8 (range 0.3 – 2.6) Gy/GBq) (*21,27*). Whole body and bone marrow absorbed doses of ^{177}Lu-FAP-2286 (0.07 and 0.05 Gy/GBq, respectively) were similar when compared to ^{177}Lu-PSMA-617 (0.04 and 0.03 Gy/GBq, respectively) (*25*) and ^{177}Lu-DOTATATE (0.05 and 0.04 Gy/GBq, respectively) (*21,26*). Absorbed doses in bone metastases were similar to those reported by Kulkarni et al. for ^{177}Lu-PSMA-617 (3.0 (range 0.5 – 10.6) Gy/GBq for ^{177}Lu-FAP-2286 vs 2.9 Gy/GBq for ^{177}Lu-PSMA-617) *(25)* and slightly lower than those reported by Violet et al. for ^{177}Lu-PSMA-617, although with overlapping range (5.3 (range 0.4 – 10.7) (*28*). The effective half-life of ^{177}Lu-FAP-2286 in the whole body (35 h) was slightly shorter than that of ^{177}Lu-PSMA-617 (40 h) *(25)* and ^{177}Lu-DOTATATE (55 h) (*21*) and slightly longer in the kidneys (81 h for ^{177}Lu-FAP-2286 vs 42 h for ^{177}Lu-PSMA-617 and 63 h for ^{177}Lu-DOTATATE) (*21,25*). Thus, although individual values may vary, the overall dose delivered by ^{177}Lu-FAP-2286 to healthy organs and tumor lesions appears comparable to that of well-known ^{177}Lu-based radiopharmaceuticals. The dosimetric analysis of the patients in this report therefore justifies prospective clinical trials to establish a safe and effective cumulative dose of ^{177}Lu-FAP-2286 as well as risk factors to be considered in diverse adenocarcinoma patients.

PTRT with ^{177}Lu-FAP-2286 appears to ameliorate symptoms in rapidly proliferating adenocarcinomas as noted by significant pain reduction in Pt 4 with liver metastases, Pt 6 with diffuse bone metastases and in Pt 5 with newly diagnosed pancreatic cancer. On the other hand, there was exacerbation of pre-existing pain or development of new local symptoms shortly after PTRT in Pt 9 (headache) and in Pt 2 after the 2nd cycle (experiencing severe abdominal complaints). Flare phenomenon after treatment with radionuclide therapy has been reported

previously *(29)*, thus the symptoms in Pt 2 and Pt 9 may potentially be related to existing metastases localized in the area of pain exacerbation.

The reasons for reduction of the radioactivity administered were pre-existing red marrow dysfunction (anemia / pancytopenia) either due to red-marrow involvement and/or status post multiple previous therapies including chemotherapy; and renal dysfunction, which potentially could result in longer whole-body residence time and increase the absorbed dose to red marrow. Therefore, the presence of these limitations prevented higher injected activity to prevent a potential additional red marrow dysfunction. G3 hematological adverse events were observed in Pt 6 (leukocytopenia) and Pt 8 (pancytopenia), correlating with an imaging evidence of diffuse bone marrow involvement. These adverse events were managed with intermittent transfusions of packed red blood cells and bone-marrow stimulation using granulocyte-colony stimulating factor. Otherwise, no severe hematological toxicity was noted in patients, despite heavy pretreatment in some including recently concluded chemotherapy (in Pts 2, 7 and 9), Immune check-point-inhibitor-therapy (Pt 10), and HER2-/bone-targeting radionuclide therapies (Pts 6, 7 and 8). In fact, the bone-marrow function in Pt 9 was not only unaffected by PTRT but improved (most probably due to termination of chemotherapy 2 weeks before start of PTRT). No organ toxicity was seen. The one instance of pre-renal, acute-on-chronic renal insufficiency in Pt 6 was manageable with intravenous fluids and resolved after 1 week.

The most likely mechanism of action of PTRT can be postulated to be the destruction of cancer-associated fibroblasts, which are the support systems for cancers, as well as a crossfire effect causing tumor-cell killing. However, progression of disease was frequently observed,

necessitating alteration of treatment strategy. The possible measures to enhance the therapeutic efficacy of PTRT are shortening of the time intervals between treatments and/or increasing the administered radioactivity. Furthermore, the evaluation of combinations with other treatments (for e.g., with a targeted therapy like PARP inhibitor, immune check-point inhibitor) stands to reason.

Other radionuclides for labeling FAP-2286 may be utilized for therapy. Although the beta-particle energy of ^{90}Y is higher than that of ^{177}Lu, the longer range of ^{90}Y-beta might increase the risk of bone-marrow and renal toxicity. However, applying a lower dosage could be appropriate as with PRRT of neuroendocrine tumors (*27*). An alpha-emitter, like ^{225}Ac, appears to be also a suitable candidate due to its high and precise energy delivery to the tumor per unit radioactivity, causing double-stranded DNA breaks (*30*). A proof-of-concept study of ^{225}Ac-FAPI-04 (as well as ^{64}Cu-FAPI-04) in FAP-expressing pancreatic cancer xenograft mouse models suggested the applicability of FAP-targeted alpha-therapy in pancreatic cancer *(31)*. The tumor half-life of FAP-2286 is much longer than FAPI-02/04, but lesser than ^{177}Lu-PSMA or -DOTA-TOC/TATE (*14, 21, 25*). In consequence, given the effective tumor half-life of ^{177}Lu-FAP-2286 (mean 44 h for bone and 32 h for single liver metastases), radionuclides like ^{67}Cu or ^{90}Y (which has the additional advantage of a higher beta particle energy) may increase exposure as compared to ^{177}Lu or ^{225}Ac. Further studies using these radionuclides would be beneficial.

The major limitation of this report is the small and heterogeneous patient population, which received as the last line of treatment PTRT with ^{177}Lu-FAP-2286 on a compassionate use basis. This was not a dose escalation study, and varying radioactivities of ^{177}Lu-FAP-2286 administered to patients makes safety and therapeutic assessment only observational. Therefore,

the preliminary, but encouraging results of this retrospective analysis must be confirmed by a prospective, randomized and controlled clinical trial.

CONCLUSION

This report provides the first clinical evidence of the feasibility of treating different aggressive adenocarcinomas with ^{177}Lu-labeled FAP-2286. High uptake and long retention in primary and metastatic tumor lesions and a reasonable toxicity profile warrant further investigation of ^{177}Lu-FAP-2286 in prospective clinical studies to systematically evaluate its safety and efficacy, and to define the patient population it would most benefit.

DISCLOSURE

C. Smerling, D. Zboralski, F. Osterkamp, A. Hoehne, U. Reineke are employees of 3B Pharmaceuticals and inventors on a patent application for FAP tracers. Other authors have nothing to disclose in respect to this study.

ACKNOWLEDGMENT

We thank Aditi Mishra, MD and the nursing staff at Zentralklinik Bad Berka for taking care of the patients mentioned in this report. We also express our gratitude to Prof. Dr. F. Giesel for referring patients for PTRT after confirmation of FAP expression on ^{68}Ga-FAPI PET/CT.

KEY POINTS

QUESTION: Is the ^{177}Lu-FAP-2286 therapy of different adenocarcinomas feasible in terms of retainability of tracer in the tumor, patient safety, and treatment efficacy?

PERTINENT FINDINGS: In a series of 11 patients with diverse advanced adenocarcinomas, ^{177}Lu-FAP-2286 was well tolerated, without any issues of urgent concern. This novel conjugate of a FAP-binding peptide demonstrated high uptake and long retention in primary and metastatic tumor lesions with a reasonable toxicity profile.

IMPLICATIONS FOR PATIENT CARE: This first-in-human use provides a direction to clinical trials for the promising and effective FAP-targeted radiopeptide therapy of various aggressive cancers.

REFERENCES

1. von Ahrens D, Bhagat TD, Nagrath D, Maitra A, Verma A. The role of stromal cancer-associated fibroblasts in pancreatic cancer. *J Hematol Oncol.* 2017;10:76.

2. Ronnov-Jessen L, Petersen OW, Bissell MJ. Cellular changes involved in conversion of normal to malignant breast: importance of the stromal reaction. *Physiol Rev.* 1996;76:69-125.

3. Shiga K, Hara M, Nagasaki T, Sato T, Takahashi H, Takeyama H. Cancer-associated fibroblasts: their characteristics and their roles in tumor growth. *Cancers (Basel).* 2015;7:2443-2458.

4. Garin-Chesa P, Old LJ, Rettig WJ. Cell surface glycoprotein of reactive stromal fibroblasts as a potential antibody target in human epithelial cancers. *Proc Natl Acad Sci U S A.* 1990;87:7235-7239.

5. Pure E, Blomberg R. Pro-tumorigenic roles of fibroblast activation protein in cancer: back to the basics. *Oncogene.* 2018;37:4343-4357.

6. Schuberth PC, Hagedorn C, Jensen SM, et al. Treatment of malignant pleural mesothelioma by fibroblast activation protein-specific re-directed T cells. *J Transl Med.* 2013;11:187.

7. Bauer S, Jendro MC, Wadle A, et al. Fibroblast activation protein is expressed by rheumatoid myofibroblast-like synoviocytes. *Arthritis Res Ther.* 2006;8:R171.

8. Varasteh Z, Mohanta S, Robu S, et al. Molecular Imaging of Fibroblast Activity After Myocardial Infarction Using a (68)Ga-Labeled Fibroblast Activation Protein Inhibitor, FAPI-04. *J Nucl Med.* 2019;60:1743-1749.

9. Hofheinz RD, al-Batran SE, Hartmann F, et al. Stromal antigen targeting by a humanised monoclonal antibody: an early phase II trial of sibrotuzumab in patients with metastatic colorectal cancer. *Onkologie.* 2003;26:44-48.

10. Scott AM, Wiseman G, Welt S, et al. A Phase I dose-escalation study of sibrotuzumab in patients with advanced or metastatic fibroblast activation protein-positive cancer. *Clin Cancer Res.* 2003;9:1639-1647.

11. Brunker P, Wartha K, Friess T, et al. RG7386, a Novel Tetravalent FAP-DR5 Antibody, Effectively Triggers FAP-Dependent, Avidity-Driven DR5 Hyperclustering and Tumor Cell Apoptosis. *Mol Cancer Ther.* 2016;15:946-957.

12. Fabre M, Ferrer C, Dominguez-Hormaetxe S, et al. OMTX705, a novel FAP-targeting ADC demonstrates activity in chemotherapy and pembrolizumab-resistant solid tumor models. *Clin Cancer Res.* 2020;26:3420-3430.

13. Jansen K, Heirbaut L, Cheng JD, et al. Selective Inhibitors of Fibroblast Activation Protein (FAP) with a (4-Quinolinoyl)-glycyl-2-cyanopyrrolidine Scaffold. *ACS Med Chem Lett.* 2013;4:491-496.

14. Lindner T, Loktev A, Altmann A, et al. Development of Quinoline-Based Theranostic Ligands for the Targeting of Fibroblast Activation Protein. *J Nucl Med.* 2018;59:1415-1422.

15. Osterkamp F, Zboralski D, Schneider E, et al., Osterkamp F, Zboralski D, Schneider E, et al.Osterkamp F, Zboralski D, Schneider E, et al.s; 3B Pharmaceuticals GmbH, assignee. COMPOUNDS COMPRISING A FIBROBLAST ACTIVATION PROTEIN LIGAND AND USE THEREOF, WO2021005125.

16. D. Zboralski, F. Osterkamp, A.D. Simmons, et al. Preclinical evaluation of FAP-2286. a peptide-targeted radionuclide therapy (PTRT) to fibroblast activation protein alpha (FAP). *Ann. Oncol.* 2020;31: S488

17. Mueller D, Breeman WA, Klette I, Gottschaldt M, Odparlik A, Baehre M, Tworowska I, Schultz MK. Radiolabeling of DOTA-like conjugated peptides with generator-produced ^{68}Ga and using NaCl-based cationic elution method. *Nat Protoc.* 2016;11:1057-1066.

18. Schultz MK, Mueller D, Baum RP, Leonard Watkins G, Breeman WA. A new automated NaCl based robust method for routine production of gallium-68 labeled peptides. *Appl Radiat Isot.* 2013;76:46-54.

19. Mueller D, Fuchs A, Leshch Y, et al. Radiolabeling and Stability of FAP- Seeking Radiopharmaceuticals for Radio-Molecular Imaging and Therapy. *J Nucl Med.* 2020;61:1129.

20. Common Terminology Criteria for Adverse Events (CTCAE): website of Cancer Therapy Evaluation Program, US Department of Health and Human Services. Published November 17, 2017; https://ctep.cancer.gov/protocoldevelopment/electronic_applications/docs/CTCAE_v5_Quick_Reference_5x7.pdf. Accessed May 22, 2021.

21. Schuchardt C, Kulkarni HR, Prasad V, Zachert C, Muller D, Baum RP. The Bad Berka dose protocol: comparative results of dosimetry in peptide receptor radionuclide therapy using (177)Lu-DOTATATE, (177)Lu-DOTANOC, and (177)Lu-DOTATOC. *Recent Results Cancer Res.* 2013;194:519-536.

22. Kratochwil C, Flechsig P, Lindner T, et al. FAPI-PET/CT: Mean intensity of tracer-uptake (SUV) in 28 different kinds of cancer. *J Nucl Med.* 2019.

23. Strosberg J, El-Haddad G, Wolin E, et al. Phase 3 Trial of (177)Lu-Dotatate for Midgut Neuroendocrine Tumors. *N Engl J Med.* 2017;376:125-135.

24. Hofman MS, Violet J, Hicks RJ, et al. [(177)Lu]-PSMA-617 radionuclide treatment in patients with metastatic castration-resistant prostate cancer (LuPSMA trial): a single-centre, single-arm, phase 2 study. *Lancet Oncol.* 2018;19:825-833.

25. Kulkarni HR, Singh A, Schuchardt C, et al. PSMA-Based Radioligand Therapy for Metastatic Castration-Resistant Prostate Cancer: The Bad Berka Experience Since 2013. *J Nucl Med.* 2016;57:97S-104S.

26. Wehrmann C, Senftleben S, Zachert C, Muller D, Baum RP. Results of individual patient dosimetry in peptide receptor radionuclide therapy with 177Lu DOTA-TATE and 177Lu DOTA-NOC. *Cancer Biother Radiopharm.* 2007;22:406-416.

27. Yadav MP, Ballal S, Tripathi M, et al. Post-therapeutic dosimetry of 177Lu-DKFZ-PSMA-617 in the treatment of patients with metastatic castration-resistant prostate cancer. *Nucl Med Commun.* 2017;38:91-98.

28. Violet J, Jackson P, Ferdinandus J, et al. Dosimetry of (177)Lu-PSMA-617 in Metastatic Castration-Resistant Prostate Cancer: Correlations Between Pretherapeutic Imaging and Whole-Body Tumor Dosimetry with Treatment Outcomes. *J Nucl Med.* 2019;60:517-523.

29. Sabet A, Khalaf F, Mahjoob S, et al. May bone-targeted radionuclide therapy overcome PRRT-refractory osseous disease in NET? A pilot report on (188)Re-HEDP treatment in progressive bone metastases after (177)Lu-octreotate. *Am J Nucl Med Mol Imaging.* 2013;4:80-88.

30. Graf F, Fahrer J, Maus S, et al. DNA double strand breaks as predictor of efficacy of the alpha-particle emitter Ac-225 and the electron emitter Lu-177 for somatostatin receptor targeted radiotherapy. *PLoS One*. 2014;7;9.

31. Watabe T, Liu Y, Kaneda-Nakashima K, et al. Theranostics Targeting Fibroblast Activation Protein in the Tumor Stroma: ^{64}Cu- and ^{225}Ac-Labeled FAPI-04 in Pancreatic Cancer Xenograft Mouse Models. *J Nucl Med.* 2020;61:563-569.

Figures

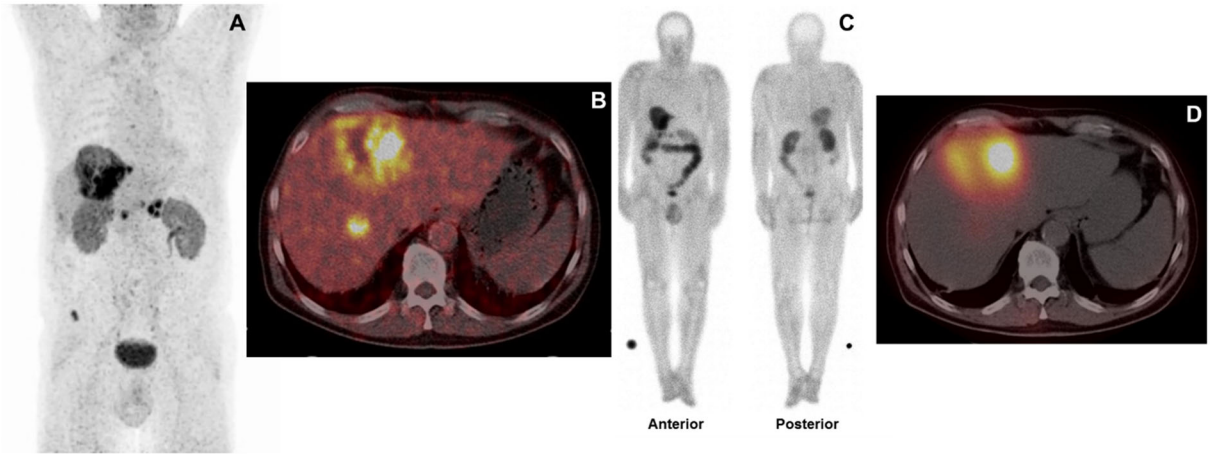

Figure 1. Pt. 4 had adenocarcinoma of the pancreatic body and hepatic, peri-pancreatic lymph node, and osseous metastases, which demonstrated a high FAP-expression on ^{68}Ga-FAP-2286 PET/CT (*A*, maximum intensity projection image, *B*, transverse fused PET/CT image). Significant uptake and late retention of ^{177}Lu-FAP-2286 was noted in the liver metastases on post-therapeutic whole-body scintigraphy in anterior and posterior view at 48 hours post injection (*C*), and the transverse fused SPECT/CT image (*D*) and. Note: due to the low resolution of ^{177}Lu for imaging as compared to PET/CT using ^{68}Ga, not all tumor sites seen on ^{68}Ga-FAP-2286 PET/CT are apparent on ^{177}Lu-FAP-2286 images.

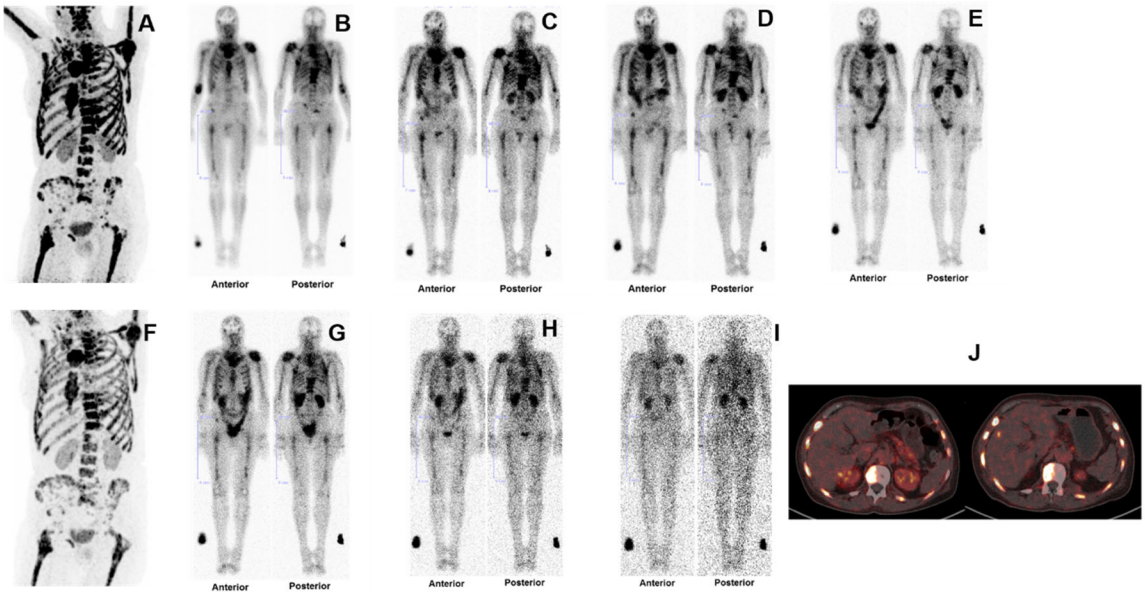

Figure 2. Pt. 6 suffered from breast cancer and presented predominantly with diffuse FAP-positive bone and bone-marrow metastases (but also lymph node metastases) on ^{68}Ga-FAP-2286 PET/CT *(A)*. The serial whole-body scintigraphy in anterior and posterior views at 3 hours *(B)*, 20 hours *(C)*, 44 hours *(D)*, 68 hours *(E)*, 92 hours *(G)*, 7 days *(H)* and 10 days *(I)* after PTRT using 2.4 GBq ^{177}Lu-FAP-2286, demonstrated uptake and retention in the metastases. The ^{68}Ga-FAP-2286 PET/CT after 8 weeks *(F)* demonstrated a mixed response – regression of bone and bone-marrow lesions, but overall progressive disease with new evidence of liver metastases (*J – fused axial ^{68}Ga-FAP-2286 PET/CT images: left, before and right, after PTRT*).

Table 1. Patient characteristics

Pt no.	Age (years)	Sex	Primary tumor	Hormone receptor status, if applicable	Metastases	Relevant previous surgery	Previous Chemotherapy regimen	Previous radionuclide therapy, if applicable, with cumulative administered radioactivity	Other relevant treatments
1	70	M	Pancreas (head and body)		LN, hep, per, oss	none	none		none
2	55	F	Pancreas (tail)		LN	Left pancreatectomy	Folfirinox, nab-Paclitaxel. Gemcitabine		none
3	78	M	Pancreas (head and tail)		Hep, per, oss	none	none		none
4	58	M	Pancreas (body)		LN, hep, oss	none	Abraxane. Gemcitabine, Capecitabine, Oxaliplatin. Irinotecan		none
5	87	M	Pancreas (body and tail)		LN, hep, per	none	none – unfit for chemotherapy		none
6	63	F	Breast	ER, PR positive, HER2 negative	Oss, LN, hep	Mastectomy	none	Lu-177 labeled HER2-ligand and bisphosphonate; 4.5 GBq (122 mCi)	Hormonal therapy, EBRT to bone metastases
7	65	F	Breast	ER, PR positive, HER2 negative	Oss, hep, brain	Mastectomy	5-FU, Epirubicin und Cyclophosphamid	Lu-177 labeled bisphosphonate; 34.4 GBq (930 mCi)	Hormonal therapy, EBRT to bone and brain metastases
8	40	F	Breast	ER, PR and HER2 positive	Oss, LN, hep, pul	Liver segment resection	Docetaxel, Cyclophosphamide	Lu-177 labeled HER2-ligand and bisphosphonate; 15.7 GBq (424 mCi)	Herceptin, EBRT to bone metastases
9	58	F	Breast		Oss, hep	Mastectomy	Docetaxel, Doxorubicin, Cyclophosphamide, Capecitabine, 5-FU, Methotrexate		EBRT to primary, hormonal therapy, Paclociclib, chemoembolization of liver metastases
10	50	F	Ovary		Pleuroperitoneal, local bowel infiltration	Palliative bowel surgery	Cisplatin, Paclitaxel, Carboplatin		Bevacizumab, Olaparib, Nivolumab,
11	61	M	Rectum		Hep, pul, LN	Resection of rectum, liver segment, and lung lobe	Folfox, 5-FU, Irinotecan		Pre-operative EBRT to primary, Panitumumab, Ramucirumab, pembrolizumab

Abbreviations – Pt: patient, no.: number, M: male; F: female, Hep: hepatic, per: peritoneal, oss: osseous, LN: lymph node, ER: estrogen receptor, PR: progesterone receptor, HER2: human epidermal growth factor receptor 2, 5-FU: 5-Fluorouracil, EBRT: external beam radiation therapy

Table 2. Safety: hematological and renal function before and 6-8 weeks after ^{177}Lu-FAP-2286 PTRT according to CTCAE v.5.0

	Hemoglobin (mmol/l)			Leukocyte count (billion cells/l)			Thrombocyte count (billion cells/l)			eGFR (ml/min/1.73 m^2)		
CTCAE v5.0 grade	Pre-therapy (n=11)	Post-1st PTRT (n=11)	Post-2nd PTRT (n=8)	Pre-therapy (n=11)	Post-1st PTRT (n=11)	Post-2nd PTRT (n=8)	Pre-therapy (n=11)	Post-1st PTRT (n=11)	Post-2nd PTRT (n=8)	Pre-therapy (n=11)	Post-1st PTRT (n=11)	Post-2nd PTRT (n=8)
CTC-1	4	5	3	2	1	0	5	3	5	0	0	0
CTC-2	2	3	4	2	2	2	0	0	0	1	1$^{\#}$	1$^{\#}$
CTC-3	0	0	0	0	0	1	0	0	0	0	0	0
CTC-4	0	0	0	0	0	0	0	0	0	0	0	0
CTC-5	NA	0	0	NA	0	0	NA	0	0	NA	0	0

NA = not applicable before ^{177}Lu-FAP-2286 PTRT (grade 5 represents death).

$^{\#}$ There was an additional non-G3 acute (on pre-existing chronic G2) pre-renal renal insufficiency after both 1st and 2nd cycles, which was reversible.

Table 3. Outcome after treatment (FAP: fibroblast activation protein, PTRT: peptide-targeted radionuclide therapy, PD: progressive disease)

Pt no.	Initial Diagnosis (month/year)	Start of PTRT / 1st cycle (month/year)	Number of FAP-PTRT cycles	Response* at 6-8 weeks after 1st cycle	Response* at 6-8 weeks after 3rd cycle, if applicable	Time to progression since initial PTRT (weeks)	Death	Cause of death	Survival since initial FAP-PTRT (months)
1	09/2019	10/2019	2	PD		8	03/2020	PD	5
2	03/2019	10/2019	2	PD		8	06/2020	PD	8
3	09/2019	10/2019	2	PD		8	12/2019	Suicide	2
4	02/2018	10/2019	2	PD		8	02/2020	PD	4
5	01/2019	12/2019	2	PD[#]		8	04/2020	PD	4
6	07/2015	10/2019	2	PD		8			Pt alive (May 2021)
7	09/2004	10/2019	2	PD		8	04/2020	PD	6
8	07/2013	10/2019	3	SD	PD	24			Pt alive (May 2021)
9	05/2008	10/2019	2	SD		20			Pt alive (May 2021)
10	03/2015	10/2019	2	PD		8	01/2020	PD	3
11	02/2009	10/2019	1	PD		6	01/2020	Broncho-pneumonia	3

*Response was evaluated by RECIST 1.1, on ^{68}Ga-FAP-2286 PET/CT (except in pt. 5) and tumor marker evaluation after 1st (in all) and 3rd (in pt. 8) PTRT cycle.

[#]Response was evaluated on RECIST 1.1 and tumor marker evaluation

Supplementary (S) tables

Supplemental Table 1 Pre-therapeutic SUVmax in representative target lesions in liver, lymph node and osseous metastases on Ga-68 FAP-2286 PET/CT (* indicates no respective target lesion with a significant uptake)

Patient ID	**SUVmax lesion 1 (Hepatic)**	**SUVmax lesion 2 (Lymph node)**	**SUVmax lesion 3 (Osseous)**	**SUVmax normal liver**
1	11.4	10	6.9	2.7
2	*	15.5	*	4.1
3	11.2	9.5	8.3	4.8
4	23.2	22.8	5.6	4
5	No Ga-68 FAP-2286 PET/CT before therapy			
6	5.1	10.9	30.1	2.1
7	6.5	7.1	16.1	3.2
8	5.4	6.6	27.6	3.7
9	*	14	8	2.8
10	*	16.6	*	2.4
11	10.6	7.7	3.6	1.4

Supplemental Table 2 Administered radioactivity of ^{177}Lu-FAP-2286, total expressed as MBq (and per kg body weight as MBq/kg in brackets)

Pt. no.	Cycle 1	Cycle 2	Cycle 3
1	5400 (63.5)	9900 (116.5)	
2	3500 (59.3)	7000 (118.6)	
3	5900 (75.6)	9000 (115.4)	
4	6300 (71.6)	9900 (112.5)	
5	5900 (118)	5100 (102)	
6	2400 (36.9)	5900 (90.8)	
7	3900 (67.2)	5900 (101.7)	
8	3400 (54.0)	6000 (95.2)	5000 (79.4)
9	3700 (38.9)	5800 (61.1)	
10	3500 (63.6)	7000 (127.2)	
11	6500 (87.8)		

Supplemental Table 3 SUVmax of tumor lesions on ^{177}Lu-FAP-2286 SPECT/CT at the respective time points

patient number	dosimetry number	lesion number	SUVmax	SPECT/CT h p.i.
1	1	1	11.35	42
4	1	1	17.19	42
6	1	1	16.97	44
6	2	1	no SPECT/CT	
6	2	2	no SPECT/CT	
7	1	1	5.93	50
7	1	2	7.96	44
7	2	1	no SPECT/CT	
8	1	1	1.89	91
8	1	2	4.51	91
8	1	3	6.06	90
8	2	1	5.61	69
8	2	2	10.37	69
8	2	3	no SPECT/CT	

Supplemental Table 4 SUVmax of kidneys on ^{177}Lu-FAP-2286 SPECT/CT

patient number	dosimetry number	SUVmax kidney right	SUVmax kidney left	SPECT/CT h p.i.
1	1	10.71	10.19	42
4	1	9.42	7.51	42
5	1	4.88	8.26	68
6	1	8.34	9,78	49
6	2		no SPECT/CT	
7	1	11.8	9.98	50
7	2	4.13	4.33	68
8	1	18.95	14.13	90
8	2	14.17	14.51	69
10	1	9.23	7.94	42

Supplemental Table 5 Dose estimations in whole body, kidneys, and red marrow

Pt. no.	Dosimetry number	Effective half-life in hours		Mean absorbed dose in Gy/GBq		Mean absorbed red marrow dose in Gy/GBq
		Whole body	Kidneys	Whole body	Kidneys	
1	1	29	61	0.05	0.6	0.04*
4	1	30	41	0.05	0.5	0.04*
5	1	28	43	0.05	0.5	0.04#
6	1	45	67	0.10	0.6	0.09*
6	2	48	161	0.10	1.4	0.07#
7	1	26	80	0.06	0.9	0.04#
7	2	25	30	0.04	0.4	0.03#
8	1	42	134	0.08	2.0	0.07*
8	2	42	160	0.09	2.0	0.06#
10	1	30	38	0.06	0.6	0.04#
^{177}Lu-FAP-2286 (10 cycles)	Mean	35	81	0.07	1.0	0.05
	Standard deviation	9	51	0.02	0.6	0.02

*dose estimation based on blood sampling

#dose estimation without blood sampling, and based on whole body activity distribution

Supplemental Table 6 Dose estimations in metastases

Pt. no.	Dosimetry no.	Lesion no.	Effective half-life in hours		Mean absorbed dose in Gy/GBq	
			Bone metastases	Liver metastases	Bone metastases	Liver metastases
1	1	1	39		3.5	
4	1	1		32		0.4
6	1	1	41		1.0	
6	2	1	44		1.0	
		2	42		3.4	
7	1	1	28		2.0	
		2	24		0.9	
7	2	1	21		1.1	
8	1	1	42		0.8	
		2	32		0.5	
		3	31		0.9	
8	2	1	120		10.6	
		2	43		2.6	
		3	60		7.2	
^{177}Lu-FAP-2286 (10 cycles)	Mean		44		3.0	
	Standard deviation		25		2.7	

Supplemental Table 7 Dose estimations in all organs

patient number	1	4	5	6	6	7	7	8	8	10	Mean	Standard
dosimetry number	1	1	1	1	2	1	2	1	2	1		deviation
Target Organ	Gy/GBq	Gy/GBq	Gy/GBq	Gy/GBq	Gy/GBq	Gy/GBq	Gy/GBq	Gy/GBq	Gy/GBq	Gy/GBq	Gy/GBq	Gy/GBq
Adrenals	0,06	0,06	0,05	0,11	0,11	0,06	0,04	0,09	0,10	0,06	0,07	0,02
Brain	0,05	0,05	0,05	0,10	0,09	0,05	0,04	0,07	0,08	0,06	0,06	0,02
Breasts				0,10	0,09	0,05	0,04	0,07	0,08	0,06	0,07	0,02
Esophagus	0,05	0,05	0,05	0,10	0,09	0,05	0,04	0,07	0,08	0,06	0,06	0,02
Eyes	0,05	0,05	0,05	0,10	0,09	0,05	0,04	0,07	0,08	0,06	0,06	0,02
Gallbladder Wall	0,05	0,05	0,05	0,10	0,10	0,06	0,04	0,08	0,09	0,06	0,07	0,02
Left colon	0,05	0,05	0,05	0,10	0,10	0,05	0,04	0,08	0,09	0,06	0,07	0,02
Small Intestine	0,05	0,05	0,05	0,10	0,10	0,05	0,04	0,08	0,09	0,06	0,07	0,02
Stomach Wall	0,05	0,05	0,05	0,10	0,10	0,05	0,04	0,08	0,08	0,06	0,07	0,02
Right colon	0,05	0,05	0,05	0,10	0,10	0,05	0,04	0,08	0,09	0,06	0,07	0,02
Rectum	0,05	0,05	0,05	0,10	0,09	0,05	0,04	0,07	0,08	0,06	0,07	0,02
Heart Wall	0,05	0,05	0,05	0,10	0,09	0,05	0,04	0,07	0,08	0,06	0,07	0,02
Kidneys	**0,6**	**0,5**	**0,5**	**0,6**	**1,4**	**0,9**	**0,4**	**2,0**	**2,0**	**0,6**	**1,0**	**0,6**
Liver	0,05	0,05	0,05	0,10	0,10	0,05	0,04	0,08	0,09	0,06	0,07	0,02
Lungs	0,05	0,05	0,05	0,10	0,09	0,05	0,04	0,07	0,08	0,06	0,06	0,02
Ovaries				0,10	0,10	0,05	0,04	0,07	0,08	0,06	0,07	0,02
Pancreas	0,05	0,05	0,05	0,10	0,10	0,06	0,04	0,08	0,09	0,06	0,07	0,02
Prostate	0,05	0,05	0,05								0,05	0,00
Salivary Glands	0,05	0,05	0,05	0,10	0,09	0,05	0,04	0,07	0,08	0,06	0,06	0,02
Red Marrow	**0,04**	**0,04**	**0,04**	**0,09**	**0,07**	**0,04**	**0,03**	**0,07**	**0,06**	**0,04**	**0,05**	**0,02**
Osteogenic Cells	0,03	0,03	0,03	0,06	0,05	0,03	0,02	0,04	0,04	0,03	0,03	0,01
Spleen	0,05	0,05	0,05	0,10	0,10	0,06	0,04	0,08	0,09	0,06	0,07	0,02
Testes	0,05	0,05	0,05								0,05	0,00
Thymus	0,05	0,05	0,05	0,10	0,09	0,05	0,04	0,07	0,08	0,06	0,06	0,02
Thyroid	0,05	0,05	0,05	0,10	0,09	0,05	0,04	0,07	0,08	0,06	0,07	0,02
Urinary Bladder Wall	0,05	0,05	0,05	0,10	0,10	0,05	0,04	0,07	0,08	0,06	0,07	0,02
Total Body	**0,05**	**0,05**	**0,05**	**0,10**	**0,10**	**0,06**	**0,04**	**0,08**	**0,09**	**0,06**	**0,07**	**0,02**

Supplemental Table 8 Safety: hematological and renal function before and 6-8 weeks after a PTRT cycle (G: grade; new adverse event or worsening of status before therapy is underlined and marked in bold; eGFR: estimated glomerular filtration rate according to the modification of diet in renal disease, MDRD, formula)

- patient 3 died after PTRT2

* There was an additional non-G3 acute (on pre-existing chronic G2) pre-renal renal insufficiency after both 1st and 2nd cycles, which was reversible.

** Pt. 10 died within 4 weeks of 2nd PTRT cycle

Pt. / PTRT cycle no.	Hemoglobin (mmol/l)		Leukocyte count (billion cells/l)		Thrombocyte count (billion cells/l)		eGFR (ml/min/1.73 m^2)	
	Pre-therapy	Post-therapy	Pre-therapy	Post-therapy	Pre-therapy	Post-therapy	Pre-therapy	Post-therapy
Pt. 1								
PTRT1	8.6	7.6	6.6	7.8	139	166	>60	>60
CTCAE v5.0 grade	G0	**G1**	G0	G0	G1	G0	G0	G0
PTRT2	7.6	6.6	7.8	7.0	166	142	>60	>60
CTCAE v5.0 grade	G1	G1	G0	G0	G0	G1	G0	G0
Pt. 2								
PTRT1	6.8	7.0	7.9	5.2	399	376	>60	>60
CTCAE v5.0 grade	G1	G1	G0	G0	G0	G0	G0	G0
PTRT2	7.0	6.5	5.2	4.9	376	300	>60	>60
CTCAE v5.0 grade	G1	G1	G0	G0	G0	G0	G0	G0
Pt. 3[#]								
PTRT1	8.9	8.7	7.8	14.1	223	321	>60	>60
CTCAE v5.0 grade	G0	G0	G0	**Non-G3 leukocytosis**	G0	G0	G0	G0
PTRT2	8.7		9.1		321		>60	
CTCAE v5.0 grade	G0		G0		G0		G0	

Pt. / PTRT cycle no.	Hemoglobin (mmol/l)		Leukocyte count (billion cells/l)		Thrombocyte count (billion cells/l)		eGFR (ml/min/1.73 m^2)	
	Pre-therapy	Post-therapy	Pre-therapy	Post-therapy	Pre-therapy	Post-therapy	Pre-therapy	Post-therapy
Pt. 4								
PTRT1	8.0	8.2	7.6	8.1	194	172	>60	>60
CTCAE v5.0 grade	G0	G0	G0	G0	G0	G0	G0	G0
PTRT2	8.7	7.5	8.1	19.2	170	155	>60	>60
CTCAE v5.0 grade	G0	**G1**	G0	**Non-G3 leukocytosis**	G0	G0	G0	G0
Pt. 5								
PTRT1	6.9	6.3	3.4	2.4	140	167	>60	>60
CTCAE v5.0 grade	G1	G1	G1	**G2**	G1	G0	G0	G0
PTRT2	6.3	6.0	3.0	2.4	167	128	>60	>60
CTCAE v5.0 grade	G1	**G2**	G1	**G2**	G0	G1	G0	G0
Pt. 6								
PTRT1	5.6	5.8	2.2	2.2	90	121	55	41
CTCAE v5.0 grade	G2	G2	G2	G2	G1	G1	G2	G2*
PTRT2	5.8	6.3	2.2	1.6	127	89	56	32
CTCAE v5.0 grade	G2	G2	G2	**G3**	G1	G1	G2	G2*

/ PTRT cycle no.	Hemoglobin (mmol/l)		Leukocyte count (billion cells/l)		Thrombocyte count (billion cells/l)		eGFR (ml/min/1.73 m^2)	
	Pre-therapy	Post-therapy	Pre-therapy	Post-therapy	Pre-therapy	Post-therapy	Pre-therapy	Post-therapy
PT. 7								
PTRT1	7.0	7.1	9.1	18.8	187	241	>60	>60
CTCAE v5.0 grade	G1	G1	G0	**Non-G3 leukocytosis**	G0	G0	G0	G0
PTRT2	7.1	6.0	8.7	8.9	241	188	>60	>60
CTCAE v5.0 grade	G1	**G2**	G0	G0	G0	G0	G0	G0
Pt.8								
PTRT1	5.9	5.9	2.8	3.7	145	140	>60	>60
CTCAE v5.0 grade	G2	G2	G2	G1	G1	G1	G0	G0
PTRT2	5.9	5.1	3.7	2.9	140	101	>60	>60
CTCAE v5.0 grade	G2	G2	G1	G2	G1	G1	G0	G0
PTRT3	5.1	4.7	2.9	1.7	103	38	>60	>60
CTCAE v5.0 grade	G2	**G3**	G2	**G3**	G1	**G3**	G0	G0

Pt. / PTRT cycle no.	Hemoglobin (mmol/l)		Leukocyte count (billion cells/l)		Thrombocyte count (billion cells/l)		eGFR (ml/min/1.73 m^2)	
	Pre-therapy	Post-therapy	Pre-therapy	Post-therapy	Pre-therapy	Post-therapy	Pre-therapy	Post-therapy
Pt. 9								
PTRT1	7.8	8.2	3.2	4.3	83	146	>60	>60
CTCAE v5.0 grade	G0	G0	G1	G0	G1	G1	G0	G0
PTRT2	8.2	8.0	4.3	4.2	146	132	>60	>60
CTCAE v5.0 grade	G0	G0	G0	G0	G1	G1	G0	G0
Pt.10**								
PTRT1	6.6	7.1	4.2	5.8	197	250	>60	>60
CTCAE v5.0 grade	G1	G1	G0	G0	G0	G0	G0	G0
PTRT2*	7.1		5.8		232		>60	
CTCAE v5.0 grade	G1		G0		G0		G0	
Pt. 11								
PTRT1	8.3	6.1	7.3	17.4	261	300	>60	>60
CTCAE v5.0 grade	G0	**G2**	G0	**Non-G3 leukocytosis**	G0	G0	G0	G0

Supplemental Table 9 Course of tumor markers in the respective tumor entities (A, before 1st PTRT; B, 4 weeks after 1st PTRT; C, 8 weeks after 1st PTRT; D, 4 weeks after 2nd PTRT; E, 8 weeks after 2nd PTRT)

1	>10000	>10000	>10000	>10000	>10000	
2	2289	2467	2819	1934	3107	
3	1671	5610	>10000	*	*	CA 19-9 (U/ml)
4	>10000	>10000	>10000	>10000	>10000	
5	310	301	231	272	365	
11	24	24	*	*	*	
6	269,8	277,7	277,7	361,9	721,2	
7	162,6	156	168	155	267,1	CA 15-3 (U/ml)
8	112,3	121,1	139	132	144	
9	36	29	31	30	39	
10	1793	1984	1826	1737	3230	CA 125 (U/ml)